## Figure legends for supplemental figures:

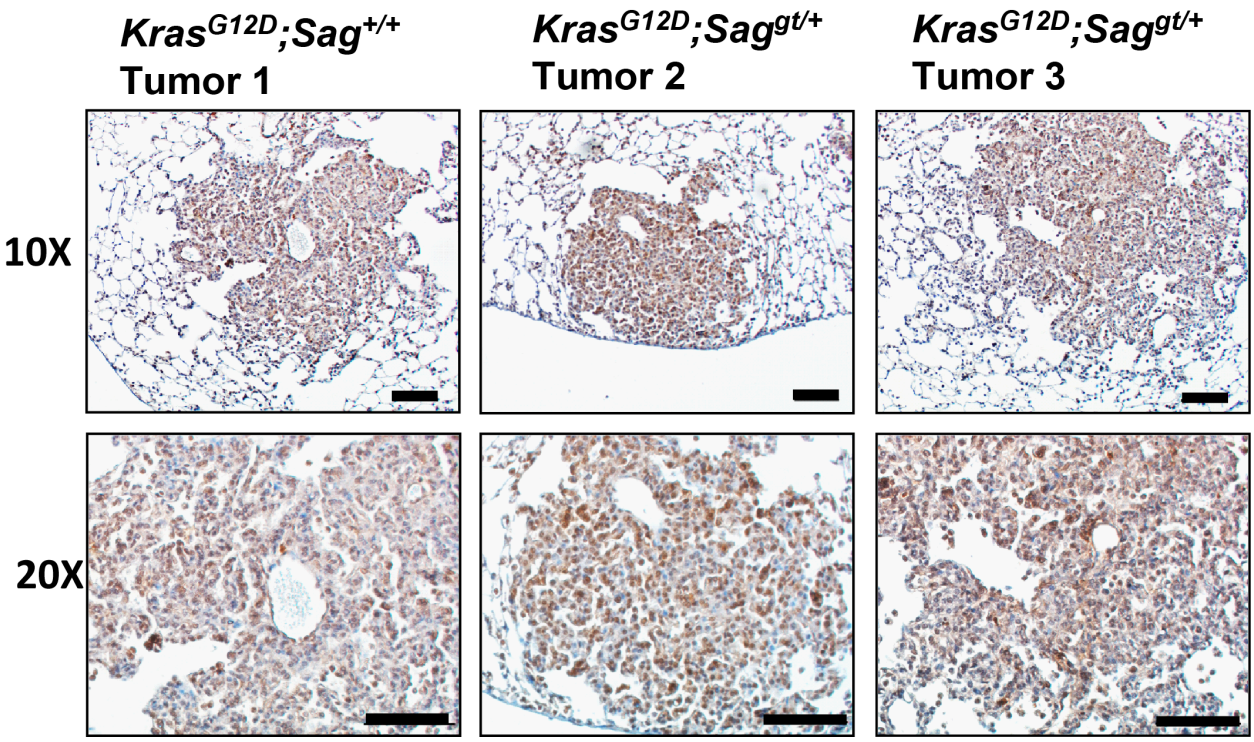


**Figure S1. Sag overexpression in lung tumors triggered by *Kras*$^{G12D}$.** Three mice with the genotype of *LSL-Kras*$^{G12D}$*;Sag*$^{+/+}$ or *LSL-Kras*$^{G12D}$*;Sag*$^{gt/+}$, respectively, were intratracheally administrated with Ad-Cre to activate *Kras*$^{G12D}$. Twelve weeks later, mice were sacrificed and their lungs harvested, fixed, sectioned and stained with anti-Sag antibody. One representative tumor from each mouse, along with adjacent normal tissues, is shown. Scale bar represents 100 μm.

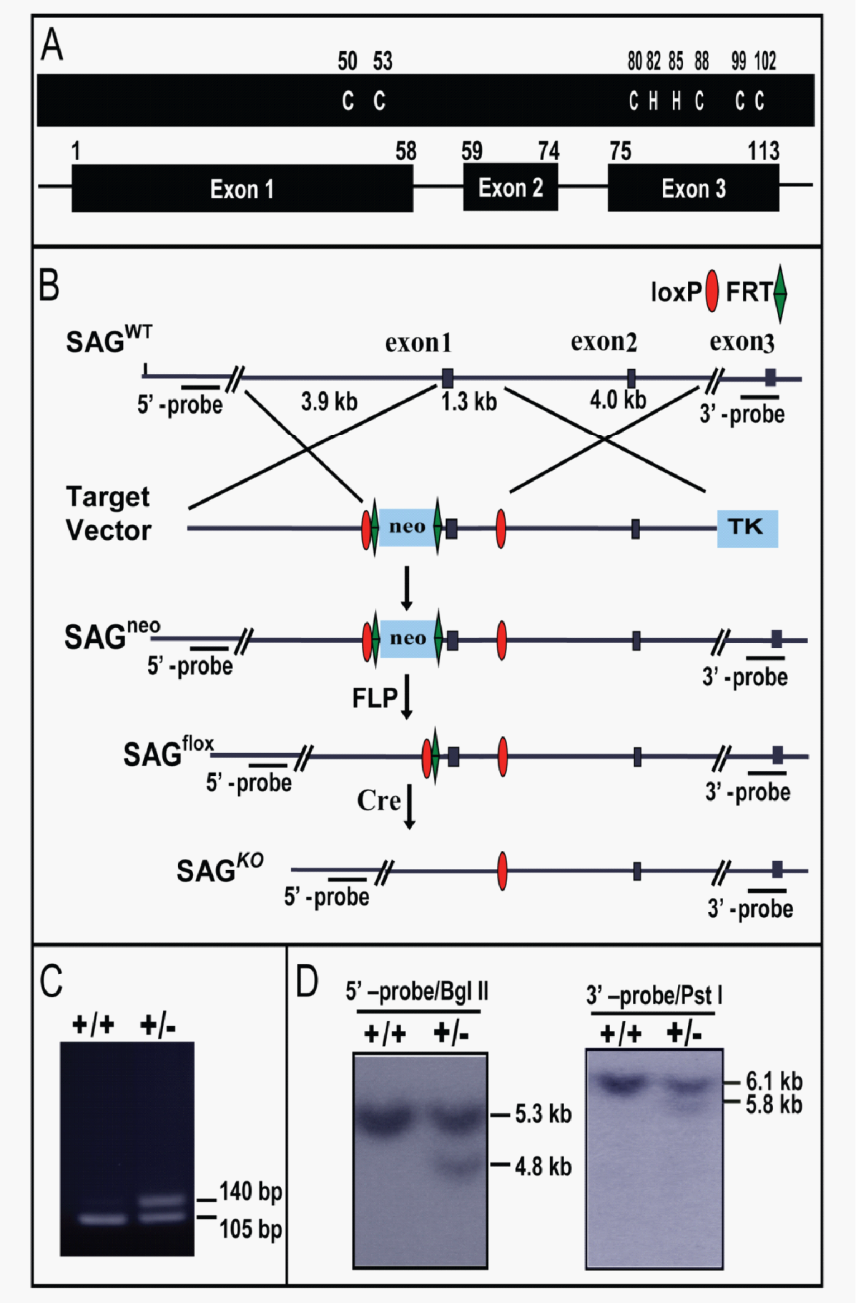


**Figure S2. Generation of the floxed and total deletion of *Sag* allele. (A).** Schematic of mouse Sag protein with the location of RING domain residues shown on top and the exon compositions and amino acids on bottom. **(B).** Targeting vector, genomic and the LoxP modified *Sag* loci. The Cre/LoxP mediated excision removes the exon 1 of the *Sag* gene, leading to a frame-shift mutation to produce a small peptide of 34 amino acids from exon 2 and part of exon 3. This peptide does not contain the functional RING domain and is a part of non-functional Sag splicing variant (hSAG-MU1) (1). **(C & D).** PCR and Southern blot of DNA from ES cells were used to identify recombinant ES clones for blastocyst injection. Similar results were obtained with the tail DNAs from germ-line-transmitted mice (data not shown).

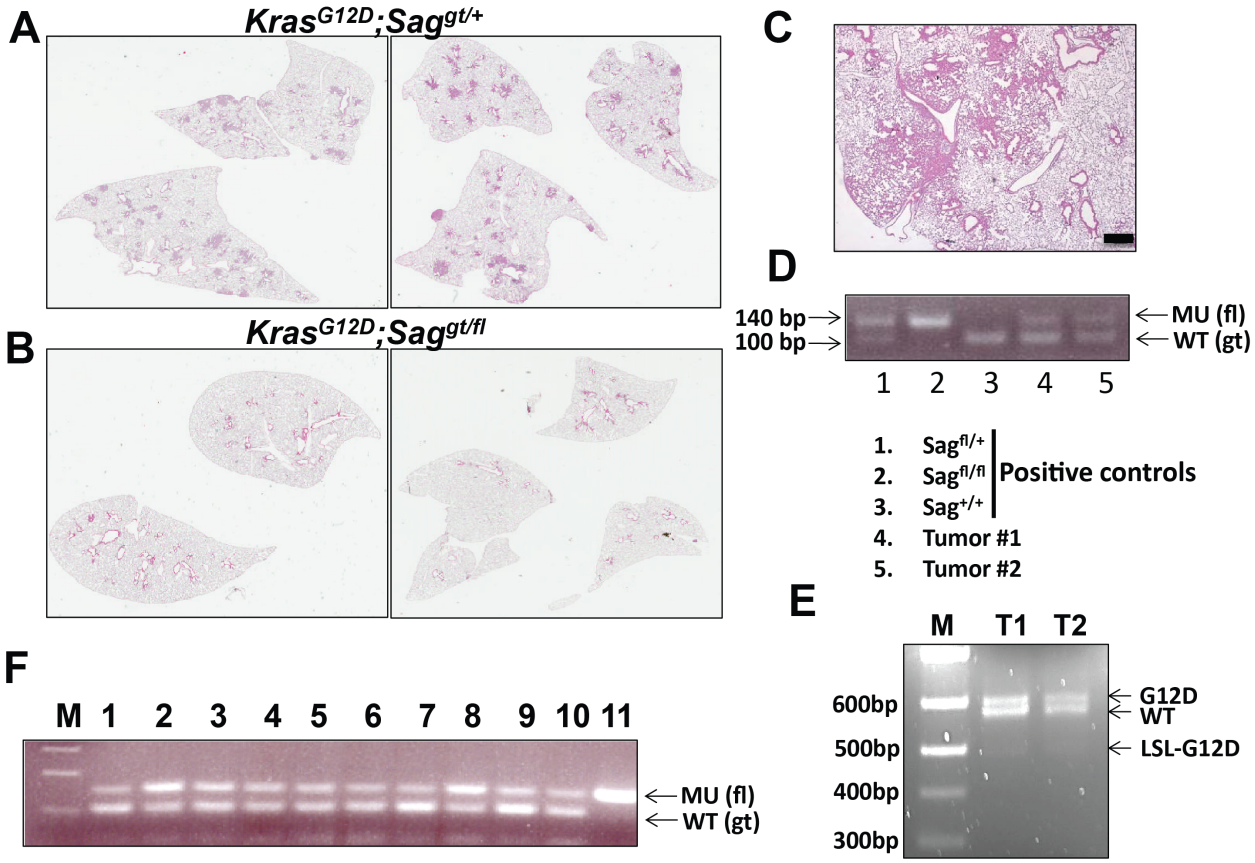


**Figure S3. *Sag* disruption inhibits *Kras*$^{G12D}$-induced lung tumor formation. (A&B).** Morphological observation of all five lobes of the lung from a representative mouse in each indicated genotype group at 12 weeks post Ad-Cre administration. (**C-F**). Incomplete *Sag* deletion and activation of Kras$^{G12D}$ in Kras$^{G12D}$-induced lung tumors**:** Morphological observation of one area of lung tissue from a mouse with the genotype of *Kras*$^{G12D}$;*Sag*$^{gt/fl}$ (C). Scale bar represents 200 μm. The PCR genotype of two independent tumors showed an incomplete deletion of *Sag*$^{fl}$ allele (D) and activation of Kras$^{G12D}$ (E), and incomplete deletion of the *Sag*$^{fl}$ allele in 10 independent tumors from 10 *LSL-Kras*$^{G12D}$;*Sag*$^{gt/fl}$ mice, 16 weeks post Ad-Cre administration (F). Note that the gene-trap (*gt*) allele was wild type, when the primer set for floxed allele was used for PCR genotyping.

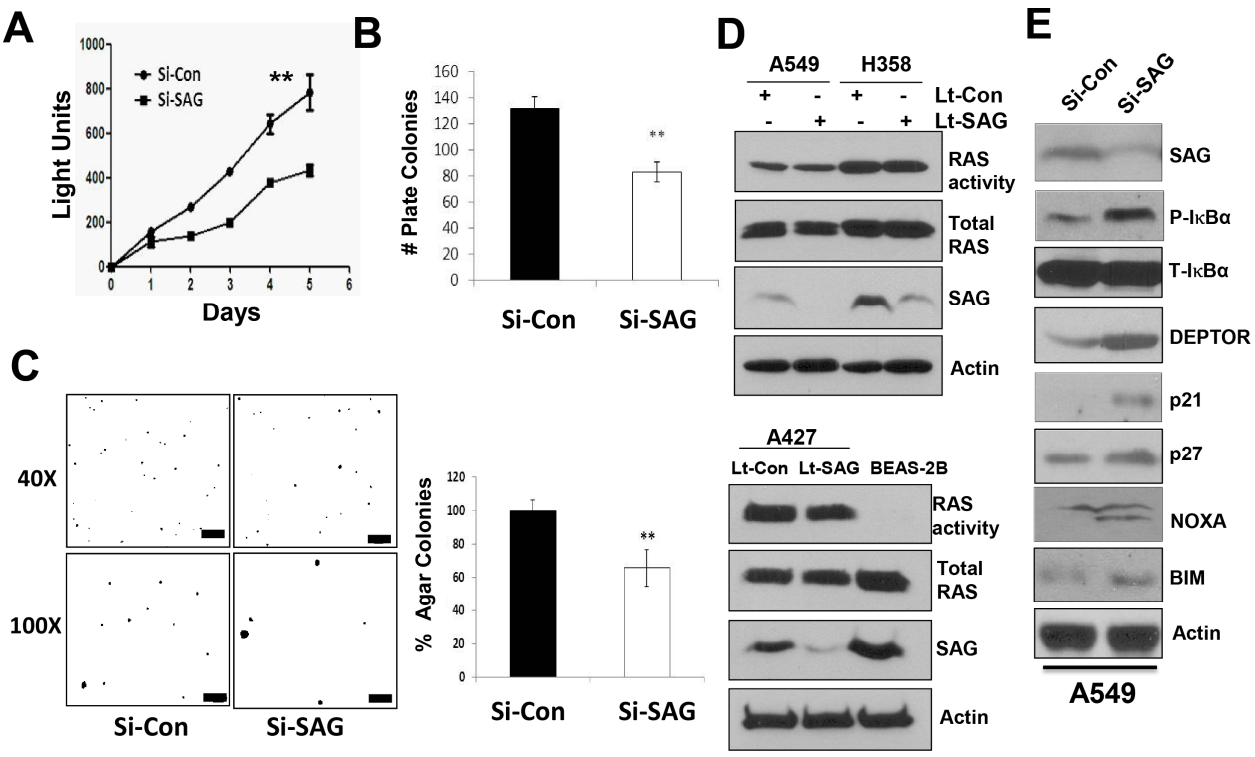


**Figure S4. SAG knockdown inhibits growth and survival of human lung cancer cells by targeting tumor suppressor substrates, but not Kras itself. (A-C).** ***SAG knockdown suppresses growth and survival:*** Human lung cancer A549 cells were transfected with siRNA oligonucleotide targeting SAG, along with scrambled siRNA control (2). Cells were tested by ATP-lite based proliferation assay, mean ± SEM (n=3), (A); clonogenic survival assay, mean ± SEM (n=3) (B); soft agar assay, mean ± SEM (n=3) (C, left panels) with quantification (C, right panel). **, $p<0.01$. (**D**). ***SAG knockdown has no effect on Kras:*** Three indicated lung cancer cell lines were infected with Lt-SAG or the Lt-Con. Lung cancer cells, along with BEAS-2B normal control, were subjected to RAF pull-down assay for RAS activity (3). **(E).** ***SAG knockdown caused the accumulation of tumor suppressor substrates:*** A549 cells were transfected with siRNA oligonucleotide targeting SAG (Si-SAG), along with Si-Con control, followed by immunoblotting using indicated Abs.

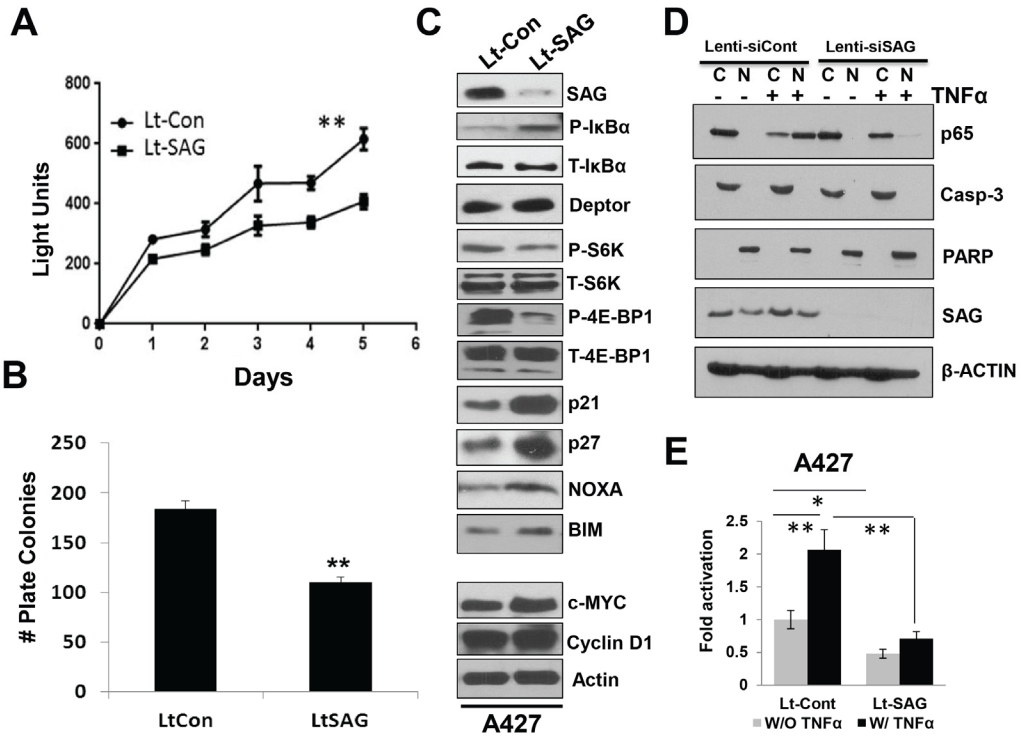


**Figure S5. SAG siRNA knockdown inhibits growth and survival of A427 lung cancer cells. (A&B)**. ***Growth of A427 cells upon SAG siRNA knockdown:*** A427 cells were subjected to lenti-virus based siRNA silencing of SAG (Lt-SAG), along with scramble siRNA control (Lt-Con). Cells were tested by ATP-lite based proliferation assay, mean ± SEM (n=3) (A); clonogenic survival assay, mean ± SEM (n=4), **, $p<0.01$ (B). (**C**). ***Accumulation of tumor suppressive proteins upon SAG knockdown:*** A427 cells were infected with Lt-SAG or Lt-Con, followed by immunoblotting using indicated Abs. (**D**). ***SAG knockdown blocks p65 nuclear translocation:*** Cells upon SAG knockdown were treated with or without TNFα (100 ng/ml) for 1 hr, followed by nuclear fractionation and immunoblotting. Caspase-3 and PARP were used to demonstrate the purity of cytoplasm and nuclear fractions, respectively. (**E**). ***Luciferase reporter based NFκB activity assay:*** Lenti-viral infected cells were transiently transfected with pNifty plasmid, along with *renilla* for transfection efficiency control. Cells were untreated or treated with TNFα (10 ng/ml) and assayed for luciferase activity. Shown are mean ± SEM (n=3), *, $p<0.05$; **, $p<0.01$.

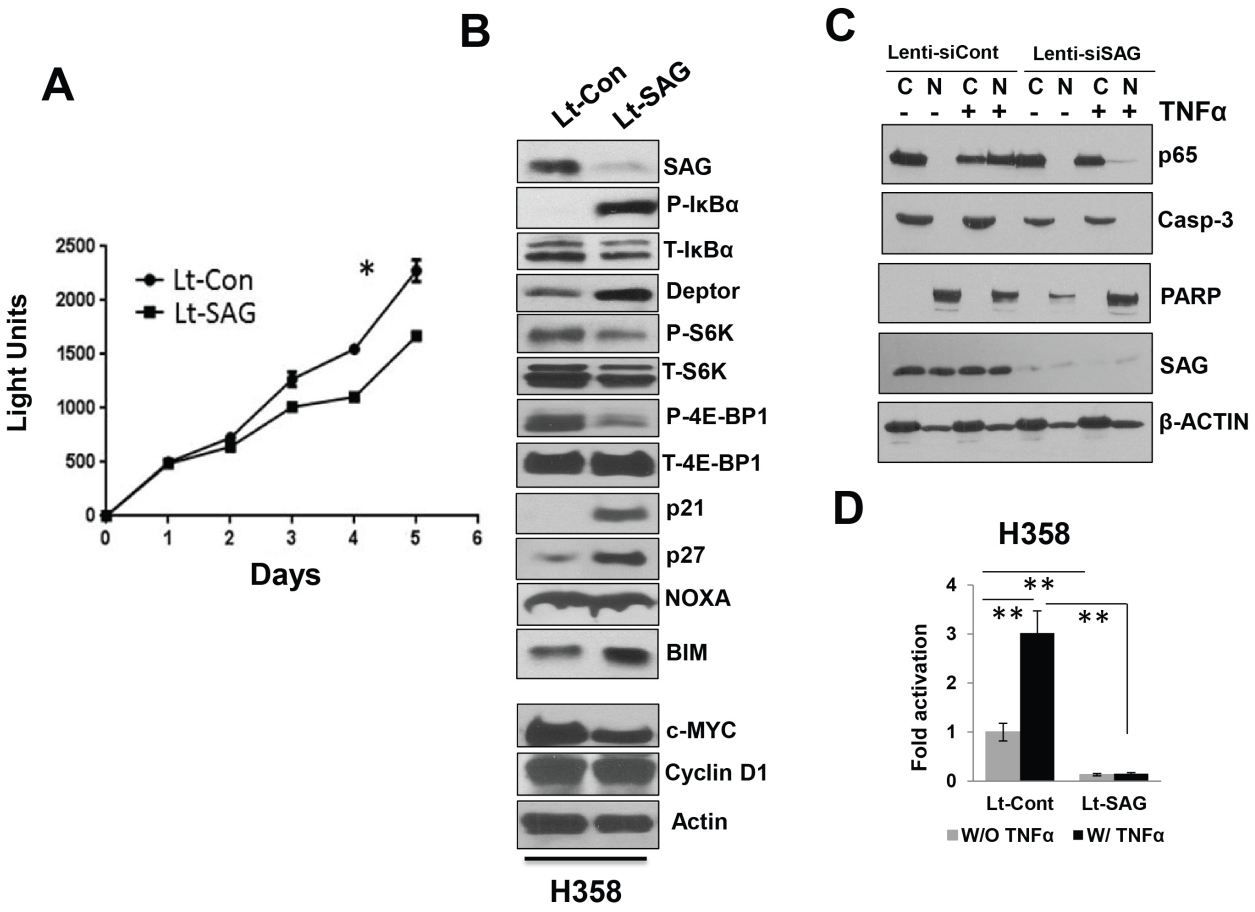


**Figure S6. SAG siRNA knockdown inhibits growth and survival of H358 lung cancer cells. (A)**. ***Growth of H358 cells upon SAG siRNA knockdown:*** H358 cells were subjected to lenti-virus based siRNA silencing of SAG (Lt-SAG), along with scramble siRNA control (Lt-Con). Cells were tested by ATP-lite based proliferation assay, mean ± SEM (n=3). (**B**). ***Accumulation of tumor suppressive proteins upon SAG knockdown:*** H358 cells were infected with Lt-SAG or Lt-Con, followed by immunoblotting using indicated Abs. (**C**). ***SAG knockdown blocks p65 nuclear translocation:*** Cells upon SAG knockdown were treated with or without TNFα (100 ng/ml) for 1 hr, followed by nuclear fractionation and immunoblotting. Caspase-3 and PARP were used to demonstrate the purity of cytoplasm and nuclear fractions, respectively. (**D**). ***Luciferase reporter based NFκB activity assay:*** Lenti-viral infected cells were transiently transfected with pNifty plasmid, along with *renilla* for transfection efficiency control. Cells were untreated or treated with TNFα (10 ng/ml) and assayed for luciferase activity. Shown are mean± SEM (n=3), **, $p<0.01$.

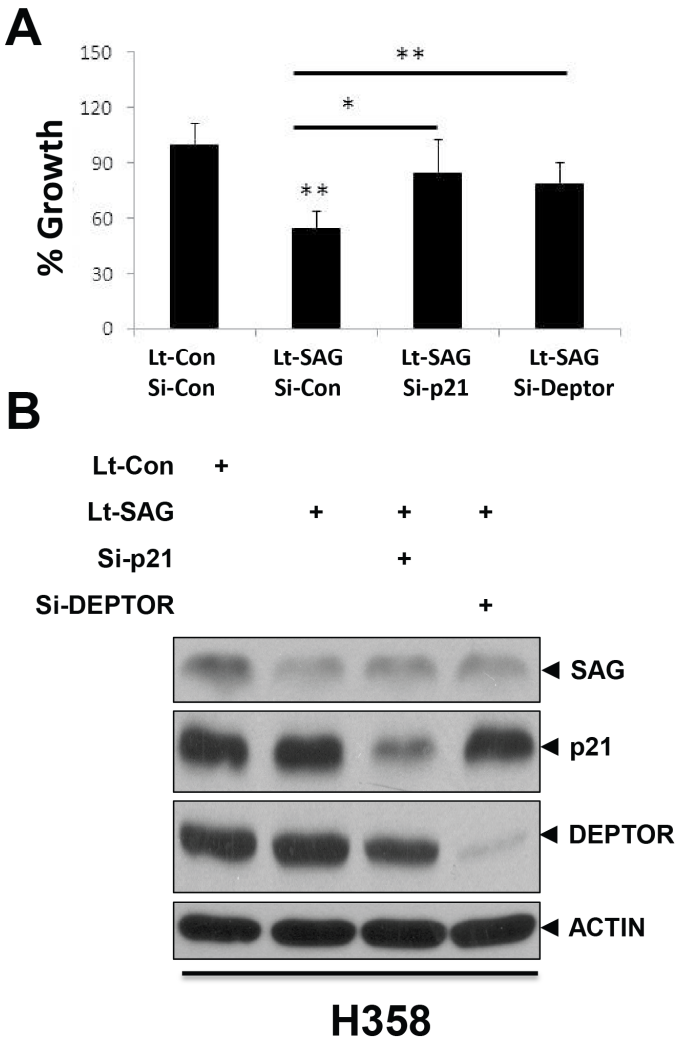


**Figure S7. Knockdown of p21 or DEPTOR partially rescues the growth suppression by SAG knockdown.** H358 cells were infected with Lt-SAG, along with the control Lt-Con. Cells were then split and transfected with siRNA oligonucleotides targeting p21 or DEPTOR, along with the silencing control (si-Con), respectively, followed by monolayer growth for 5 days. Cell proliferation was measured by ATP-lite assay. Shown (top) is mean ± SEM (n=3); *, $p<0.05$; **, $p<0.01$. Cell pellets were subjected to immunoblotting using indicated Abs (bottom).

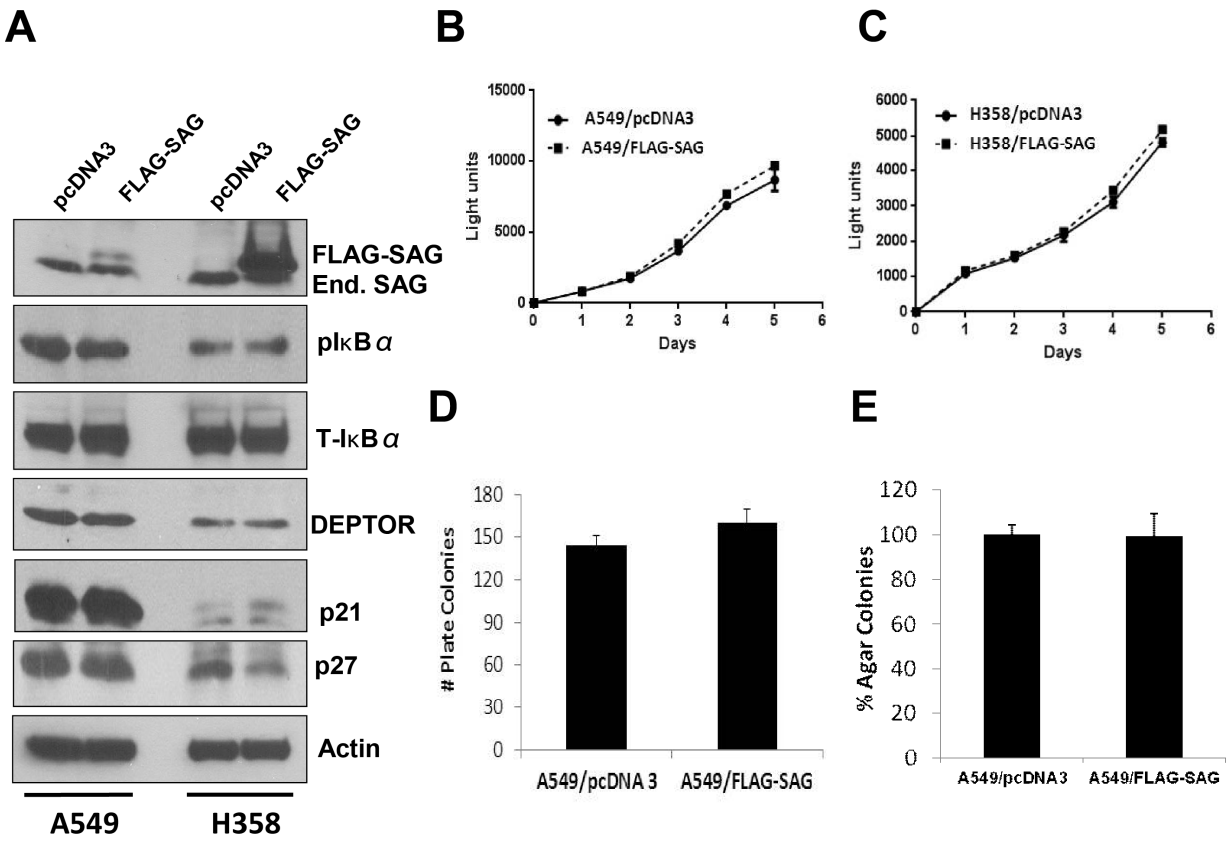


**Figure S8. No effect of SAG overexpression in A549 and H358 cells.** FLAG-tagged SAG construct, along with pcDNA3 vector control was transfected into A549 and H358 cells, followed by G418 selection for about 2 weeks. Drug-resistant stable clones were pooled and subjected to immunoblotting with indicated Abs (**A**), and assays for cell proliferation (**B&C**), clonogenic survival (**D**), and soft agar (**E**).

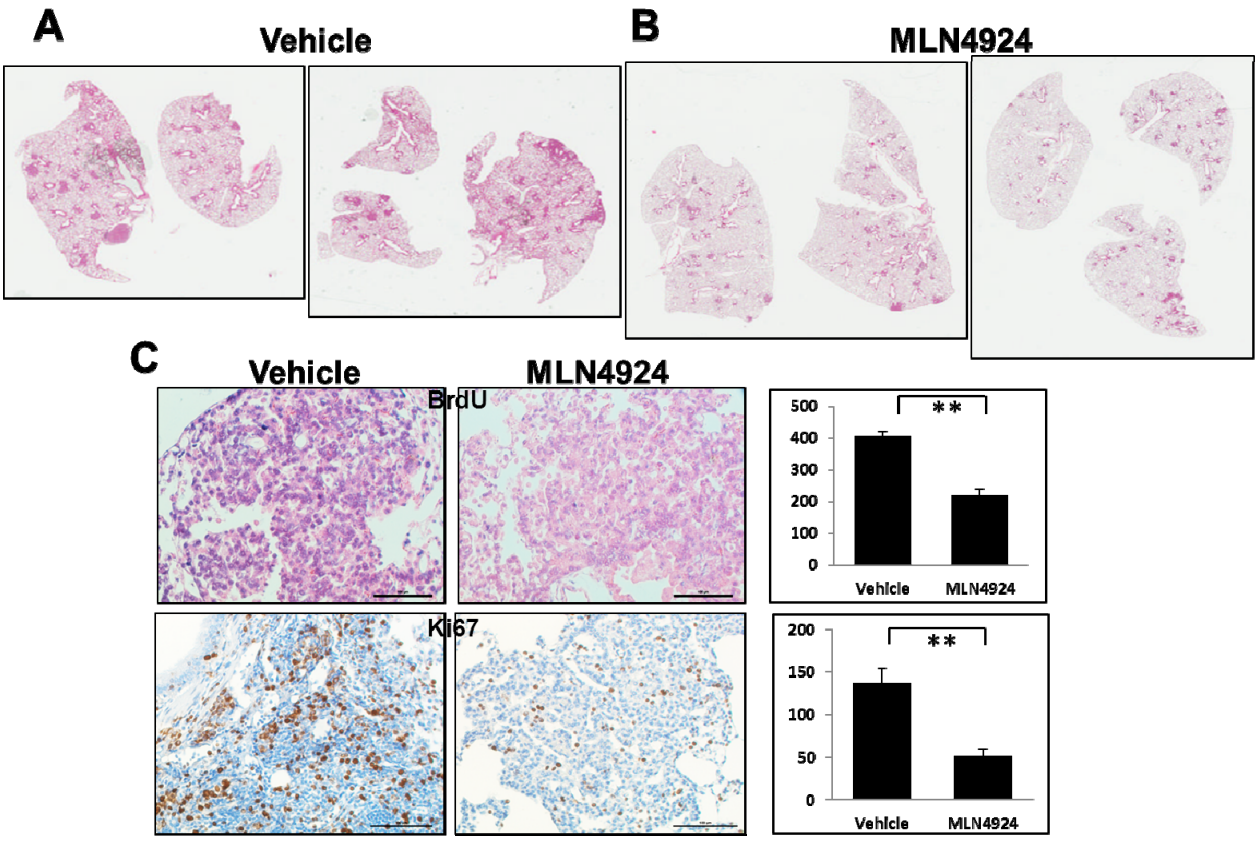


**Figure S9. MLN4924 inhibits *Kras*$^{G12D}$-induced lung tumorigenesis by suppression of proliferation.** Mice were infected via intranasal administration of Ad-Cre. Twelve weeks later, mice were randomly selected to receive the vehicle or MLN4924 at non-toxic dose (s.c 60 mg/Kg, 5 days per week) for 4 weeks (**A&B**) or 1 week (**C**). Shown are morphological observation of all five lobes of the lung tissues from one representative *Kras*$^{G12D}$;Sag$^{+/+}$ mouse, either with vehicle control or MLN4924 treatment for 4 weeks (A&B). Mice were injected with BrdU 2 hrs post last MLN4924 injection in 1-week dose regimen. Two hrs later, mice were euthanized, lung removed for fixation, section and staining with BrdU or Ki67. Shown are representative images from three independent mice in each group (C, left). Staining quantification: positively stained cells were counted out of a total of 500 cells in average from three independent tumors derived from three mice per group (C, right). Bar size = 100 μm, ** $p$<0.01.

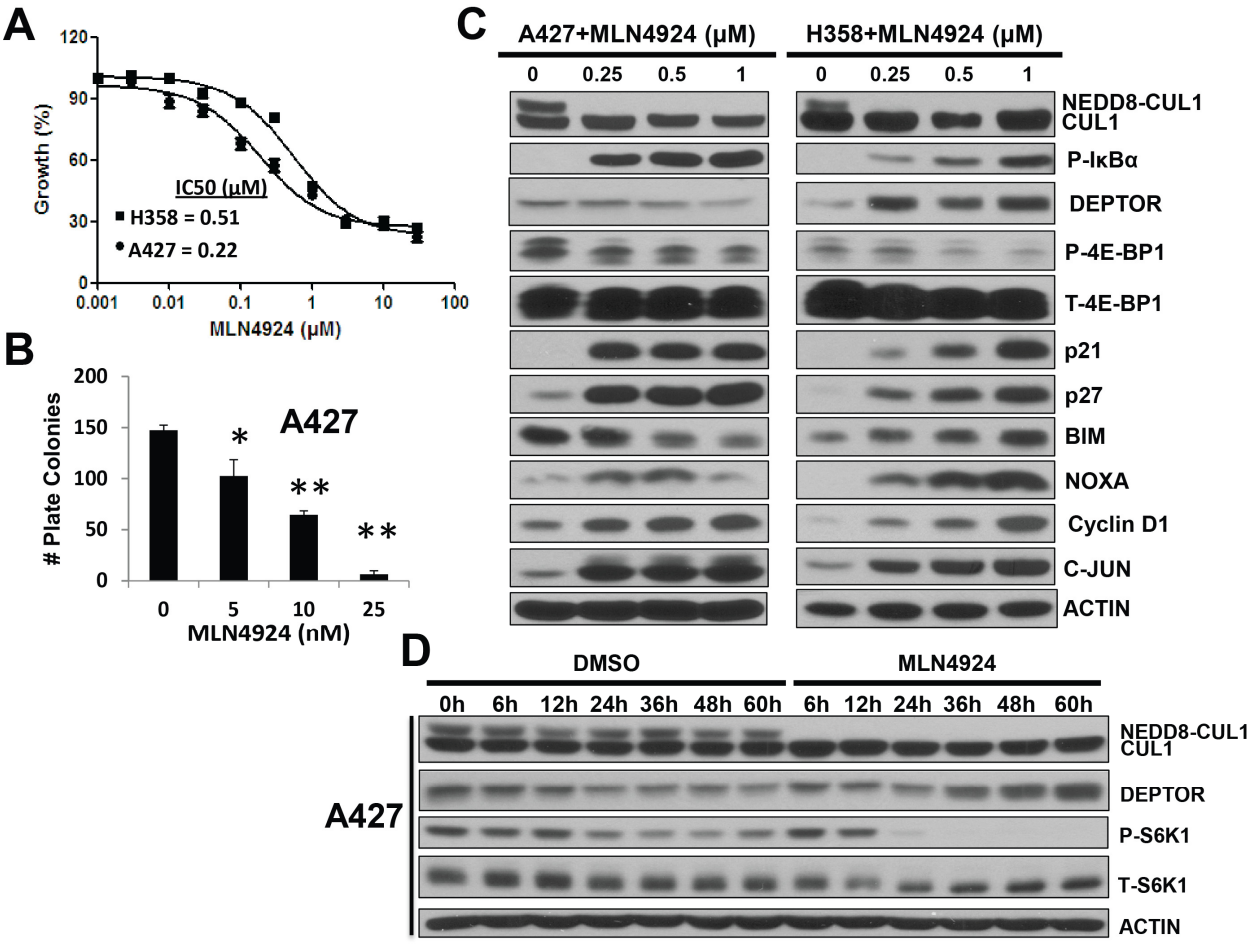


**Figure S10**. **MLN4924 suppresses growth of lung cancer cells by targeting NFκB and mTOR pathways and accumulating tumor suppressor substrates. (A&B).** A427 and H358 human lung cancer cells were treated with MLN4924 at indicated concentrations. Growth suppression effect was tested by monolayer growth, mean ± SD (n=2) (A), and clonogenic survival (A427 cells only), mean ± SD (n=2) (B). *, $p<0.05$; **, $p<0.01$. (**C**). Accumulation of tumor suppressive proteins: A427 and H358 cells were treated with indicated concentrations of MLN4924 for 24 hrs, followed by immunoblotting using indicated Abs. (**D**). Time-dependent DEPTOR accumulation and mTORC1 inactivation: Cells were treated with 1 μM MLN4924, along with DMSO control, for indicated periods of time, followed by immunoblotting.

**Table S1. RBX1 expression vs. overall survival of patients: Cox regression analysis**

| | | |
|---|---|---|
| ***Univariate Analysis: (n=442)*** | | |
| **Predictor** | **HR (95% CI)** | **P-Value** |
| **RBX1** | 1.12(0.79,1.58) | 0.531 |
| | | |
| ***Multivariate Analysis (n=434):*** | | |
| **Predictor** | **HR(95% CI)** | **P-Value** |
| **RBX1** | 1.06(0.76,1.47) | 0.747 |
| Stage* | | |
| II vs. I | 2.81(2.00,3.96) | <.0001 |
| III vs. I | 4.73(3.25,6.880) | <.0001 |
| Age | 1.03(1.01,1.04) | 0.0004 |
| Gender (Female vs. male) | 0.80(0.60,1.07) | 0.132 |
| Grade | | |
| 2 vs. 1 | 0.94(0.57,1.54) | 0.803 |
| 3 vs. 1 | 1.22(0.74,2.01) | 0.442 |

**References for supplemental figures**


1. Sun, Y. 1999. Alteration of SAG mRNA in human cancer cell lines: Requirement for the RING finger domain for apoptosis protection. *Carcinogenesis* 20:1899-1903.

2. Gu, Q., Tan, M., and Sun, Y. 2007. SAG/ROC2/Rbx2 is a novel activator protein-1 target that promotes c-Jun degradation and inhibits 12-O-tetradecanoylphorbol-13-acetate-induced neoplastic transformation. *Cancer Res* 67:3616-3625.

3. Tan, M., Zhao, Y., Kim, S.J., Liu, M., Jia, L., Saunders, T.L., Zhu, Y., and Sun, Y. 2011. SAG/RBX2/ROC2 E3 Ubiquitin Ligase Is Essential for Vascular and Neural Development by Targeting NF1 for Degradation. *Dev Cell* 21:1062-1076.